



Systemic study of solvent-assisted active loading of gambogic acid into liposomes and its formulation optimization for improved delivery

Wei-Lun Tang^a, Wei-Hsin Tang^a, Andras Szeitz^a, Jayesh Kulkarni^b, Pieter Cullis^b, Shyh-Dar Li^{a,*}

^a Faculty of Pharmaceutical Sciences, University of British Columbia, Vancouver, British Columbia, V6T 1Z3, Canada

^b Department of Biochemistry and Molecular Biology, University of British Columbia, Vancouver, British Columbia, V6T 1Z3, Canada

ARTICLE INFO

Article history:

Received 21 December 2017

Received in revised form

1 March 2018

Accepted 2 March 2018

Available online 3 March 2018

Keywords:

Ammonium copper acetate gradient

Gambogic acid

Remote loading

Insoluble weakly acidic drugs

Liposomes

Miscible solvents

ABSTRACT

The solvent-assisted active loading technology (SALT) was developed for encapsulating a water insoluble weak base into the liposomal core in the presence of 5% DMSO. In this study, we further examined the effect of various water miscible solvents in promoting active loading of other types of drugs into liposomes. To achieve complete drug loading, the amount of solvent required must result in complete drug solubilization and membrane permeability enhancement, but must be below the threshold that induces liposomal aggregation or causes bilayer disruption. We then used the SALT to load gambogic acid (GA, an insoluble model drug that shows promising anticancer effect) into liposomes, and optimized the loading gradient and lipid composition to prepare a stable formulation (Lipo-GA) that displayed >95% drug retention after incubation with serum for 3 days. Lipo-GA contained a high drug-to-lipid ratio of 1/5 (w/w) with a mean particle size of ~75 nm. It also displayed a prolonged circulation half-life (1.5 h vs. 18.6 h) and enhanced antitumor activity in two syngeneic mice models compared to free GA. Particularly, complete tumor regression was observed in the EMT6 tumor model for 14 d with significant inhibition of multiple oncogenes including HIF-1 α , VEGF-A, STAT3, BCL-2, and NF- κ B.

© 2018 Elsevier Ltd. All rights reserved.

1. Introduction

Doxil[®] was the first FDA approved liposomal formulation. Since then, a number of liposomal formulations, such as Marqibo[®] (vincristine liposome), Onivyde[®] (irinotecan liposome), and Vyxeos[®] (cytarabine and daunorubicin co-encapsulated liposome), have been approved for cancer treatment [1–4]. These liposomal products are prepared by active loading, for which the solubilized amphiphilic drug can diffuse through the lipid membrane to form impermeable complexes with the counter ions inside the aqueous core of liposomes. This method provides high drug encapsulation efficiency, minimal drug loss (<5%) during manufacturing, and increased stability for storage and in blood circulation. However, this technology can only be used for amphipathic drugs that exhibit both good aqueous solubility and membrane permeability, such as doxorubicin. Poorly water soluble drugs are normally loaded into the lipid bilayer with limited capacity and poor drug retention, leading to burst drug release and little improvements in efficacy

and safety [5,6]. We have previously showed that a water insoluble weak base drug (staurosporine, STS) could be actively loaded into the liposomal aqueous core via an ammonium gradient in the presence of 5% DMSO [7]. It was hypothesized that DMSO could solubilize STS in the loading mixture (STS and liposomes in buffer) and promote the drug permeation into the liposomal core for active loading. This drug loading method was named **S**olvent-assisted **A**ctive **L**oading **T**echnology (SALT). To the best of our knowledge, this was the first report disclosing a technology allowing active and complete loading of an insoluble compound into the inner aqueous core of liposomes at a high drug-to-lipid ratio (0.2, w/w). This liposomal STS (Lipo-STS) displayed prolonged pharmacokinetics (PK), enhanced safety, and increased efficacy against the tumor in mice compared to free STS (dissolved in Tween80/ethanol/saline). However, it remains unclear whether the SALT can be applied to loading of different types of drugs, whether various solvents can be used in this system, and what the roles of the solvents are in promoting the drug loading (solubilization vs. liposomal membrane permeability). These fundamental questions need to be systematically studied to better understand the SALT system, tailor the loading for each drug and develop a solid platform technology for active loading of insoluble drugs. To study the first question, we

* Corresponding author. 5519-2405 Wesbrook Mall, Vancouver, BC, V6T 1Z3, Canada.

E-mail address: shyh-dar.li@ubc.ca (S.-D. Li).

selected gambogic acid (GA, weak acid, water solubility <5 µg/mL) as the model compound to test whether the SALT can be applied to loading of different types of drugs. We also took the advantage that GA is soluble in a variety of water miscible solvents to examine the range of solvents that can be used for liposomal drug loading. Finally, we examined the solvent effect on solubilization of GA, aggregation/disruption of liposomes, and GA loading efficiency. The results were compared and analyzed to delineate the solvent effect in promoting GA loading into liposomes, and the optimal range of solvent content in the loading mixture was identified for each solvent to achieve complete loading of GA.

GA, a natural product extracted from the *Garcinia hanburyi* tree, has been demonstrated to exhibit potent anticancer activity against a wide range of cancers both *in vitro* and *in vivo* [8–10]. GA inhibits cancer cells through multiple mechanisms, including cell cycle arrest, apoptosis, anti-angiogenesis, anti-metastasis, and anti-inflammation [11–16]. GA can also synergistically enhance efficacy of other chemotherapeutic agents [17–19]. However, the clinical application of GA has been limited by its poor water solubility (<5 µg/mL) and short half-life (<4 h) [20,21]. Strategies, including PEG conjugation and passive encapsulation of GA into the hydrophobic compartment of nanoparticles, have been developed to increase the drug solubility, but the improvements in PK and efficacy were only minimal to moderate, probably due to *in vivo* instability of the formulations with burst drug release [22–26]. In general, liposomes have been utilized to increase drug solubility by loading insoluble drugs in the lipid bilayer. However, the bilayer loading is often unstable with limited capacity, leading to instability of the formulation and/or burst drug release in blood circulation. The SALT might offer a solution to this challenge by forming stable drug complexes in the liposomal core. To advance this technology, the second part of this study was focused on optimizing the loading gradient and lipid composition for preparing stable Lipo-GA that retained the drug when incubated with serum. Finally, the optimal Lipo-GA was compared with free GA for their hemolytic activity, PK, and antitumor efficacy to demonstrate the utility of the SALT.

2. Methods and materials

2.1. Materials

GA was purchased from Guangzhou Boji Medical Biotechnological Co. (Tianhe District, Guangzhou, China). Phospholipids were obtained from Avanti Polar Lipids (Alabaster, AL). Sepharose CL-4B, and Sephadex G-50 were purchased from Fisher Scientific (Ottawa, ON, Canada). Human and sheep red blood cells (RBCs) for hemolysis test were purchased from Innovative Research (Novi, MI). DiI18(5); 1,1'-dioctadecyl-3,3',3'-tetramethylindodicarbocyanine (DiI) & SuperScript III reverse transcriptase were purchased from ThermoFisher Scientific (Mississauga, ON, Canada). Primers for RT-PCR were purchased from Integrated DNA Technologies (Toronto, Ontario, Canada). All other chemical reagents and organic solvents were of analytical grade and obtained from Sigma-Aldrich (Oakville, ON, Canada).

2.2. Maintenance of cell lines

B16F10 murine melanoma and EMT6 murine breast cancer cells were purchased from Cedarlane (Burlington, ON, Canada), and cultured in DMEM media supplemented with 10% FBS in T75 flasks in an incubator maintained at 37 °C with 5% CO₂.

2.3. Instrumentation and experimental analysis for GA analysis

A Waters ACQUITY Ultra Performance Liquid Chromatography

(UPLC) H-Class System equipped with a photodiode array (PDA) detector was used to determine the solubility of GA and the concentrations of GA in liposomal formulations. GA solutions and Liposomal GA formulations were diluted with acidified methanol (3 vol% acetic acid) prior to sample injection. Two µL of the diluted sample was injected and then separated through a BEH-C18 column (2.1 × 50 mm) using a gradient mobile phase. The mobile phase consisted of solvent A: acetonitrile with 0.1 vol% formic acid and solvent B: MilliQ water with 0.1 vol% formic acid. The flow rate was 0.4 mL/min with the following gradient: 0 min: A/B (10/90), 1.8 min: A/B (85/15), 2.7 min: A/B (15/85), 4 min: A/B (10/90). The concentration of GA was determined by integrating the chromatographic peak area detected at a wavelength of 360 nm using the Empower 3.0 software. The mobile phase was sterile filtered. The U(H)PLC-MS/MS system used for measuring GA in biological samples was composed of an Agilent 1290 Infinity Binary Pump, a 1290 Infinity Sampler, a 1290 Infinity Thermostat, and a 1290 Infinity Thermostatted Column Compartment (Agilent, Mississauga, ON, Canada). The U(H)PLC system was connected to an AB Sciex QTrap[®] 5500 hybrid linear ion-trap triple quadrupole mass spectrometer equipped with a Turbo Spray source (AB Sciex, Concord, ON, Canada). The mass spectrometer was operated in negative ionization mode. Chromatographic analysis was conducted using a Waters Acquity UPLC BEH-C18, 1.7 µm 2.1 × 100 mm column, which was protected by a Waters Acquity UPLC BEH-C18 VanGuard guard column (1.7 µm, 2.1 × 5 mm) (Waters Corp., Milford, MA). The mobile phase consisted of Solvent A: water with 2.5 mM ammonium formate (AF), and solvent B: acetonitrile with 2.5 mM AF. The mobile phase initial conditions were solvent A (10 vol%) and solvent B (90 vol%), which was ramped to solvent A (5 vol%) by 1.3 min and held until 3.0 min followed by an equilibration with solvent A (10 vol%) and solvent B (90 vol%) for 2 min. The flow rate was 0.2 mL/min, and the injection volume was 15 µL with a total run time of 6.0 min. The mobile phase flow was diverted to the waste before 1.4 min and after 4.1 min during the chromatographic run. GA was quantified using a daughter ion (m/z 628.17 → 583.1) and the internal standard (IS; ursolic acid, m/z 455.5), and GA concentration in biological samples was determined by comparing the results from the standard samples containing known concentrations of GA (dissolved in 12 mM arginine solution) or liposomal GA (Lipo-GA) (25–750 ng/mL). The chromatographic retention time for GA and the I.S. were 2.49 min and 2.41 min, respectively. Data were acquired using the Analyst 1.5.2. software.

2.4. Liposome preparation and drug loading

All liposomal formulations were composed of phospholipids (DSPC or DOPC) and cholesterol with or without DSPE-mPEG2K with various ratios, and were prepared with the thin film hydration method. Briefly, technique lipid film was hydrated with one of the internal phases listed in Table 1, and extruded through a series of polycarbonate filters with pore sizes ranging from 0.2 to 0.08 µm, using a Lipex Extruder (Transferra, Vancouver, BC, Canada) to obtain small unilamellar vesicles with a mean diameter between 70 and 120 nm. Basified copper acetate (250 mM) or copper sulfate (250 mM) was prepared by titrating the pH to 9.5 using 28–30% (vol) ammonium hydroxide solution.

The temperature applied during the extrusion depended on the phase transition temperature of the phospholipid component. DOPC liposomes were extruded at room temperature, whereas DSPC liposomes were extruded at 65 °C. Particle size and zeta potential were measured with a Zetasizer (Nano-ZS, Malvern Instruments, Malvern, UK). The external phase was exchanged by passing the liposomes through a Sephadex G-50 column pre-equilibrated with one of the external phases listed in Table 1

Table 1
Examples of trapping agents and miscible solvents for drug loading.

Gradient preparation for drug loading		Drug loading		After loading
	Internal phase	External phase	Miscible solvent	External buffer
Weak acid	Trapping agent			HEPES buffered saline (HBS, pH 7.5)
Gambogic acid (GA, M.W. 628.76)	200 mM Calcium (II) formate 150 mM Magnesium (II) gluconate 250 mM Copper(II) acetate (pH 5.2) 250 mM Basified copper acetate (pH 9.5) 250 mM Basified copper sulfate (pH9.5)	50 mM borate buffer (pH 8.5)	DMSO, DMF, EtOH, MeOH, acetonitrile, acetone, 1,4-dioxane, NMP	
Weak base	Trapping agent			
Staurosporine (STS, M.W. 466.53)	300 mM Ammonium sulfate	100 mM acetate buffer (pH 5.5)	DMSO, 1,4-dioxane	

containing 25 mM EDTA followed by another passage over a G-50 column pre-equilibrated with the EDTA free external phase. The liposomes containing a loading gradient were then mixed with a drug in the presence of a miscible solvent (2–50% for GA & 2–70% for STS) selected from Table 1 at room temperature for 30 min at a drug-to-total lipid ratio of 0.1 (w/w). Un-encapsulated drug and the miscible solvent were removed by dialysis or passage through a Sephadex G-50 column equilibrated with HEPES buffered saline (HBS, pH 7.5). Residual DMSO content in liposomes was measured by an UPLC method as described previously [48].

2.5. Determination of the minimal amount of solvent required for complete solubilization of 1 mg/mL GA or STS

GA and STS were dissolved in 50 mM borate buffer (pH 8.5) and 100 mM acetate buffer (pH 5.5), respectively, at 1 mg/mL in the presence of 0–10 vol% of a solvent selected from Table 1. The solution/suspension was centrifuged at 14,000 rpm for 20 min, and the supernatant was analyzed for drug concentration by the UPLC-UV method described in Method 2.2.

2.6. The solvent impact on liposome integrity

Preformed liposomes composed of DSPC/Chol (55/45, molar ratio) were incubated in HBS containing 2–75% of a solvent selected from Table 1 at 10 mg total lipid/mL for 30 min at room temperature. The liposome integrity was analyzed by measuring the size and the polydispersity index (PDI) with a Zetasizer particle analyzer.

2.7. The solvent impact on drug loading

Preformed liposomes (DSPC/Chol, 55/45 mol%) containing either the Mg²⁺ gradient (150 mM magnesium gluconate) or ammonium gradient (300 mM ammonium sulfate) were mixed with either GA or STS, respectively, at 1 mg drug/mL with a drug-to-lipid ratio of 0.1 (w/w) in the presence of 0–60 vol% of a miscible solvent selected from the list in Table 1. The mixture was incubated for 30 min, followed by purification using a Sephadex G-50 spin column pre-equilibrated with HBS. The loading efficiency was determined by the following equation, where the drug concentration was measured by the UPLC-UV method and the DSPC concentration was measured by the Stewart assay [27]

$$\text{Loading efficiency (\%)} = \frac{[\text{Drug}]_{\text{purified}} / [\text{DSPC}]_{\text{purified}}}{[\text{Drug}]_{\text{initial}} / [\text{DSPC}]_{\text{initial}}} \times 100\%$$

2.8. In vitro drug retention analysis

Various liposomal GA formulations labeled with DID (1% mol) were mixed with heat-deactivated FBS (1:1 v:v) at 800 µg GA/mL, and incubated at 37 °C over a period of 48 h. At selected time points, 300 µL of the mixture was collected, and passed through a Sepharose CL-4B column pre-equilibrated with HBS to remove released GA, and 150 µL of the liposomal fraction was collected. The percentage of drug retention was calculated by the formula shown below, where [GA] was determined by the UPLC method, and [DID] was estimated by absorbance at 650 nm by a microplate reader.

$$\text{Drug retention (\%)} = \frac{([\text{GA}]_{\text{post-purification}} / [\text{DID}]_{\text{post-purification}}) / ([\text{GA}]_{\text{pre-purification}} / [\text{DID}]_{\text{pre-purification}})}{\times 100\%}$$

2.9. Cryo-transmission electron microscopy (Cryo-TEM) analysis

Cryo-TEM imaging was performed using a modification to previously described methods [28,29]. Liposomes were concentrated to ~15–25 mg/mL total lipid and vitrified using a Mark IV Vitrobot (FEI, Hillsboro, OR). Frozen grids were stored under liquid nitrogen until imaged. Grids were further prepared to support AutoLoader function on a FEI Titan Krios fitted with the Falcon III direct electron detector (FEI, Hillsboro, OR). Images were obtained at 47,000× magnification and a nominal under focus of 1–2 µm. All imaging was performed at the Life Sciences Institute (UBC, Vancouver, BC).

2.10. Hemolysis test

Free GA formulation was prepared as reported previously [22] by dissolving 2 mg GA in 1 mL of 12 mM arginine solution. GA formulations were then diluted with PBS and mixed with red blood cells (human or sheep, final 1.5 vol%) at a concentration of 40 µg GA/mL, representing the estimated C₀ for the *in vivo* study. The sample was incubated for 1 h at 37 °C, followed by centrifugation at 2500 rpm for 10 min. The absorbance (OD) of the supernatant at 545 nm was determined by a microplate reader. TritonX-100 (2.5 vol%) was used as a positive control. The percentage of hemolysis was calculated as follows:

$$\text{Hemolysis (\%)} = \frac{OD_{\text{sample}} - OD_{\text{blank control}}}{OD_{\text{positive control}} - OD_{\text{blank control}}} \times 100$$

2.11. Animal models

Female BALB/c and C57/BL6 mice (18–20 g) were purchased

from The Jackson Laboratory (Bar Harbor, ME). All the *in vivo* studies were conducted in accordance with the established experimental protocols approved by the Animal Care Committee of the University of British Columbia (Vancouver, BC, Canada). BALB/c and C57BL6 mice were implanted s.c. with EMT6 and B16F10 (2×10^5 cells in 50 μ L media) into the shaved right lateral flank, respectively. One to two weeks later, mice were randomly divided into 4 groups when tumor size reached 70–110 mm³. Each group was comprised of 5–6 mice for PK and antitumor efficacy studies described below.

2.12. PK study

The EMT-6 tumor-bearing mice were i.v. injected with free GA or Lipo-GA at 10 mg GA/kg, and plasma was collected at different time points. Drug extraction from plasma was performed by modifying the previous method [30]. One hundred μ L of plasma was mixed with 200 μ L MeCN containing IS (20 ng/mL), 2 μ L 3 M HCl, and 100 μ L 2 M ammonium sulfate. The mixture was then vortex for 2 min and centrifuged at 9500 rpm for 6 min. Fifteen μ L of the top phase was analyzed using the U(H)PLC-MS/MS method described above. PK parameters were obtained by analyzing the plasma profile with Phoenix WinNonlin[®] software (Princeton, NJ) using the non-compartmental model.

2.13. *In vivo* antitumor activity

Free GA (4 mg GA/kg) and Lipo-GA (4 or 20 mg GA/kg) were given intravenously when the tumor size reached 70–110 mm³. In the control group, the mice were i.v. treated with 100 mg lipids/kg of empty liposomes (lipid dose equivalent to that of Lipo-GA at 20 mg GA/kg). The therapeutic efficacy was assessed by monitoring tumor size and body weight every day. The tumor size was measured by a LCD digital caliper, and calculated as (tumor length) \times (tumor width)² \times 0.52. The tumor size and body weight of mice were monitored daily until the control group reached the end point (\sim 1500 mm³). In EMT6 tumor model, 3 mice from each group were euthanized 3 d post-administration to obtain tumor tissue for Real Time-Polymerase Chain Reaction (RT-PCR) analysis of selected genes. At the experimental endpoint for the EMT6 tumor model, mice were euthanized for tumor harvest. Tumors were incubated in 10 vol% formalin in PBS at room temperature for 2 days followed by paraffin-embedded section and H&E or immunohistochemical staining for Ki67, CD31, and NF- κ B p65. Image analysis was conducted with the ImageScope software using Positive Pixel Count algorithm. Image analysis output was positive pixel counts divided by the area analyzed. All data was normalized against the control.

2.14. RT-PCR

Total RNA from tumor was extracted with the Qiagen RNeasy Plus Mini Kit according to the manufacturer's instruction. Complementary DNA (cDNA) was reverse-transcribed using the First-Strand Synthesis System (Invitrogen). cDNA was amplified with specific primers (Supplementary Table 1) using a Fast SYBR[™] Green Master Mix (ThermoFisher Scientific) and a StepOnePlus[™] RT-PCR System (Applied Biosystems). 18s rRNA was used as the endogenous control. the comparative CT Method ($\Delta\Delta$ Ct) was used to calculate the relative fold difference of each gene expression.

2.15. Statistical analysis

Significant differences were determined by the Student's *t* test using GraphPad Prism 6.0 (La Jolla, CA). Difference between two groups with a *p* value < 0.05 was considered statistically significant.

All data are express as mean \pm standard deviation.

3. Results and discussion

3.1. Solvent effect on drug solubility, liposome integrity and drug loading

We have previously demonstrated that by including 5 vol% DMSO in the mixture of staurosporine (STS, solubility in water <2 μ g/mL) and liposomes containing an ammonium sulfate gradient, STS could be actively loaded and stably encapsulated inside the liposomal core at a high drug-to-lipid ratio of 0.2 (w/w) [7]. It was observed that 5 vol% DMSO completely solubilized STS and facilitated permeation of STS molecules through the lipid bilayer to form complexes inside the aqueous core, evidenced by cryo-transmission electron microscopy. In this report, we performed systemic studies on the SALT, aiming to answer three questions. First, can the SALT be applied to other types of drugs in addition to weak base compounds? Second, are other water miscible solvents compatible with the SALT system? Third, how can solvents promote drug loading?

We strategically selected GA as the model drug to perform the study as this weak acid drug belongs to a different class of compounds, and is soluble (>20 mg/mL) in a wide range of water miscible solvents. We hypothesized that a water miscible solvent can help dissolve GA in the exterior phase and increase the membrane permeability, thereby promoting GA molecules to penetrate the lipid bilayer at room temperature and then form complexes with the metal ion to get trapped inside the liposomes. However, since the solvent could dissolve the lipids, if the solvent concentration exceeds a limit, the liposomal membrane may become too leaky to retain the loading gradient. It was also hypothesized that the concentration limit for each solvent for disrupting the bilayer would be different. To confirm the hypotheses, we first determined the minimal amount of solvent required to completely dissolve 1 mg/mL of GA in borate buffer, and studied the solvent tolerability of the DSPC/Chol liposomes against different solvents at a range of concentrations by monitoring the particle size change. A total of 8 solvents were tested, and it was found that 2 vol% of solvent was needed for complete solubilization of GA in borate buffer at 1 mg/mL, except for dioxane, 5 vol% was required (Table 2 & Supplementary Fig. 1A). In the solvent tolerability test (Table 2 & Supplementary Table 2), DMSO, DMF, and MeOH did not cause liposomal particle size change up to a concentration of 50 vol%. However, for DMSO and DMF at 50 vol%, the mixture turned blurry, possibly due to precipitation of the salts. EtOH, MeCN, acetone and dioxane did not aggregate liposomes up to a concentration of 20 vol%. The liposomes only tolerated NMP up to 5–10 vol%, but at 10 vol% the mixture turned blurry, again possibly due to insolubility of the salts. Measuring the particle size is a robust method to estimate the tolerability of the liposomal bilayer against different concentrations of solvents. However, it is understood that disruption of the liposomal loading gradient could occur at a lower solvent concentration (than the result from the solvent tolerability data), and the increase of membrane permeability could begin at an even lower solvent content. Nevertheless, the solvent tolerability data provide quick information of the upper limit for a solvent to be used in the SALT.

The fluorescent dye leakage assay is a standard method to measure liposomal membrane permeability [31,32]. However, when a miscible organic solvent was present in the system, it was very challenging to study membrane leakage using this method. In fact, this assay was first employed, but the data were not conclusive as the fluorescence intensity of the released dye was affected by the organic solvent. Additionally, both solvent type and solvent amount

Table 2
Summary of the solvent effect on drug solubility, liposomal aggregation and drug loading. DSPC/Chol liposomes (55/45, mol%) with a loading gradient were used. Drug loading for 1 mg/mL of GA was performed at a D/L of 1/10, w/w) for 30 min at room temperature. The loading gradients for GA was 150 mM magnesium gluconate.* high drug loading = loading efficiency >90%. Data = mean \pm SD (n = 3), N.D. = not determined.

Miscible solvent	Minimal % of solvent for Complete solubilization	Optimal range to maintain high drug loading (%) [*]	Minimal % of solvent to cause size change	Gambogic acid (GA)										
				Loading efficiency (%)										
				0	1	2	5	7	10	20	50			
DMSO	2	5–20	70	1.55 \pm 0.57	41.36 \pm 2.12	81.26 \pm 3.30	97.11 \pm 2.02	N.D.	101.1 \pm 2.24	93.51 \pm 2.78	76.83 \pm 1.52			
DMF	2	5–20	70	1.55 \pm 0.57	41.86 \pm 2.86	67.31 \pm 3.36	99.64 \pm 3.18	N.D.	101.42 \pm 1.16	94.31 \pm 4.76	76.38 \pm 8.04			
MeOH	2	5–10	70	1.55 \pm 0.57	35.41 \pm 3.82	67.43 \pm 4.39	99.53 \pm 3.70	91.66 \pm 2.08	89.35 \pm 5.50	63.56 \pm 2.09	38.27 \pm 4.87			
EtOH	2	5–7	50	1.55 \pm 0.57	42.57 \pm 3.12	85.37 \pm 2.49	94.67 \pm 5.24	89.44 \pm 1.61	78.91 \pm 3.58	71.47 \pm 5.31	N.D.			
MeCN	2	5	50	1.55 \pm 0.57	35.26 \pm 2.61	70.57 \pm 4.91	101.12 \pm 3.51	83.70 \pm 1.45	66.65 \pm 3.08	56.30 \pm 5.70	N.D.			
Acetone	2	5	50	1.55 \pm 0.57	24.95 \pm 4.51	67.54 \pm 3.35	97.40 \pm 2.15	83.47 \pm 3.61	78.69 \pm 5.69	69.11 \pm 4.68	N.D.			
NMP	2	7–10	20	1.55 \pm 0.57	52.28 \pm 3.26	68.92 \pm 2.36	85.74 \pm 5.16	98.46 \pm 2.62	100.73 \pm 3.02	74.29 \pm 3.78	N.D.			
14-dioxane	5	7–10	50	1.55 \pm 0.57	12.73 \pm 2.64	81.68 \pm 5.26	85.91 \pm 1.81	99.04 \pm 3.67	94.63 \pm 3.94	56.91 \pm 7.72	N.D.			

in the system displayed significant impact on the fluorescence measurement, making the data difficult to interpret and conclude. Thus, we measured the loading efficiency to reflect the solvent effect on the membrane permeability, shown to be robust.

We performed liposomal loading of GA in the presence of a range of solvents at various solvent concentrations, and the results are shown in Table 2. It is established that complete GA loading could be achieved with all the tested solvents, and the optimal solvent concentration must exceed the minimal solvent content for complete drug solubilization. However, such solvent concentration cannot surpass the optimal threshold beyond which the solvent leads to liposomal aggregation (Table 2 & Supplementary Fig. 1B). Similar results were also obtained with a weak base drug, STS (Supplementary Table 3). Nevertheless, the optimal range of concentration for the same solvent was different for different drugs (GA vs. STS). This may be attributed to the different ability of the liposomes for retaining different loading gradients. We then further demonstrated that this method could be used to load a variety of other drugs into liposomes, including artesunate, prednisolone hemisuccinate, and quercetin (Supplementary Table 4). Our results indicate that: first, the SALT can be applied to a wide range of compounds; second, a variety of water miscible solvents are compatible with the SALT and can be used to facilitate drug loading; third, to achieve complete drug loading, the solvent concentration needs to slightly exceed that for complete drug solubilization, suggesting that the solvent acts both on solubilizing the drug as well as increasing the membrane permeability for effective drug permeation at room temperature.

3.2. Optimization of Lipo-GA formulation

The next aim of this study was to optimize the liposomal formulation for enhanced therapy of cancer to demonstrate the utility of SALT. We first compared GA loading efficiency of the DSPC/Chol/DSPE-mPEG2K liposomes with different loading gradients, including magnesium gluconate, calcium formate, copper acetate (pH 5.2), and basified copper acetate (pH 9.5). As depicted in Fig. 1A, liposomes with all loading gradients achieved complete drug loading in the presence of 5 vol% DMSO at a drug-to-total lipid of 1/5 w/w. We then measured the drug retention in the liposomes composed of various loading gradients in the presence of 50% serum. Burst drug leakage was found in all the liposomal formulations (>60% in 2.5 h, Fig. 1B); however, among these, the basified copper acetate gradient retained the drug the most. The data indicate that Cu²⁺ exhibited the highest activity forming stable complexes with GA among these different metal ions. Increasing the pH in the copper acetate loading gradient further increased the GA retention, and this could be due to that at the basic pH, GA was effectively ionized inside the liposomes and became less membrane permeable to leak out. We then employed the basified copper acetate as the loading gradient and altered the lipid composition to prepare different liposomal formulations and compared their drug retention in 50% serum. As shown in Fig. 1C, decreasing the content of Chol in PEGylated DSPC liposomes improved GA retention from 40% to 68% (45–0 mol% of Chol) in the first 2.5 h. However, there was no significant improvement in drug retention 12 h post incubation (>70% drug leakage for all formulations). Reducing the Chol content in the lipid composition has been shown to improve retention for hydrophobic drugs, such as idarubicin [33]. It was speculated that hydrophobic drugs would exhibit decreased interaction with low-Chol liposomal membrane, resulting in decreased drug leakage. We then compared formulations prepared with either DOPC, an unsaturated phospholipid, or DSPC, a saturated phospholipid. As depicted in Fig. 1D, the DOPC formulation (DOPC/Chol/DSPE-mPEG2K, 85/10/5, mol%) retained >95% drug after 24 h

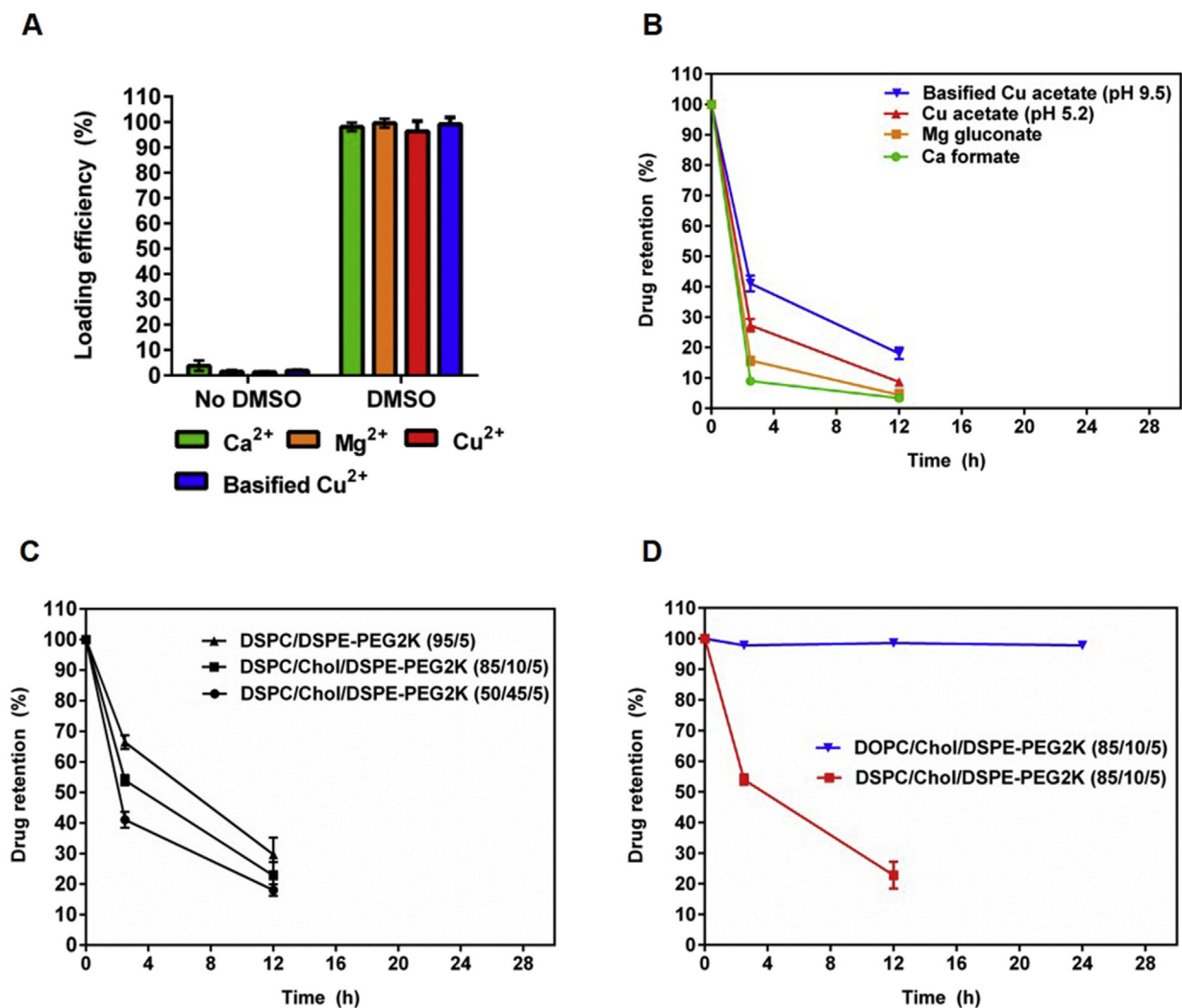


Fig. 1. Optimization of liposomal formulations for GA. (A) GA loading into liposomes composed of DSPC/Chol/DSPE-mPEG2K (50/45/5, mol%) containing various trapping agents in the absence or presence of 5 vol% DMSO. (B) GA retention in liposomes containing different loading gradients when incubated in 50% FBS at 37 °C. (C) GA retention in liposomes containing various amounts of Chol when incubated in 50% FBS at 37 °C. (D) GA retention in liposomes composed of either DOPC or DSPC when incubated in 50% FBS at 37 °C.

incubation in 50% FBS without significant size change (Supplementary Fig. 2), while its DSPC counterpart showed ~80% drug leakage in 12 h. This result was somewhat surprising as liposomes composed of a saturated lipid with an increased transition temperature have been shown to retain doxorubicin better compared to an unsaturated lipid [34]. The reason that the DOPC formulation offered enhanced GA retention relative to the DSPC formulation remains unclear. However, it has been discovered that DOPC could form more flexible liposomes to trap hydrophobic molecules more efficiently relative to saturated lipids [35]. It is worth mentioning that our data also showed that the SALT could be applied for a variety of liposomal formulations for active drug loading, including non-PEGylated liposomes (DSPC/Chol), high and low Chol content liposomes, DSPC liposomes, and DOPC liposomes. The physical characteristics of the optimized Lipo-GA were summarized in Table 3, and the residual DMSO in the final formulation was <0.55 ppm. The formulation was used for the following studies in comparison with free GA. We also examined the morphology of Lipo-GA using Cryo-TEM imaging. As shown in Fig. 2, Lipo-GA displayed bilamellar conformation with an electron-dense structure inside the liposomal core. These two features of structure have been shown with other liposomal drug formulations with a copper gradient [36,37], suggesting copper ions formed complexes with

GA and contributed to the lipid bilayer rearrangement as well as enhanced drug retention.

3.3. Hemolysis test

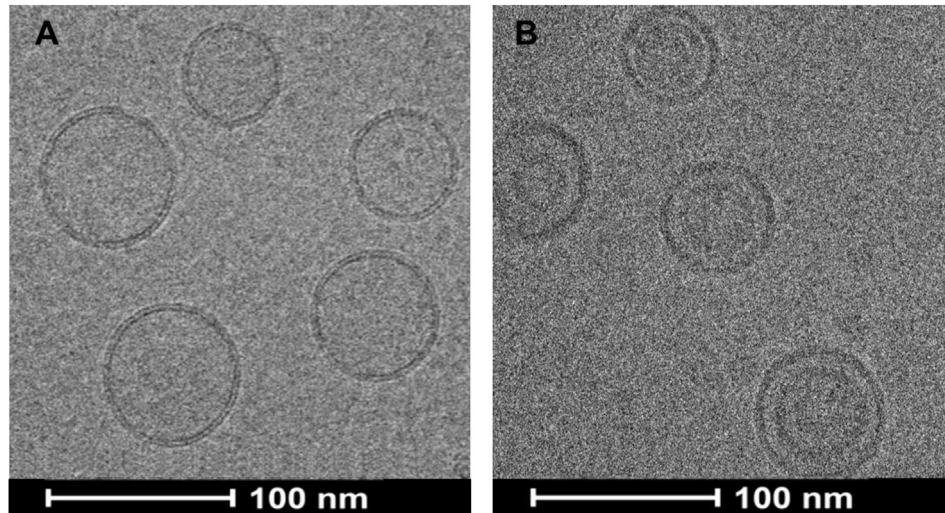
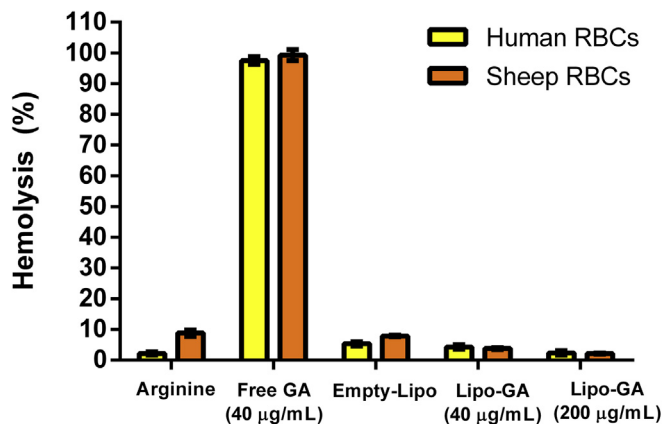
GA has been shown to induce apoptosis in erythrocytes, which could induce significant toxicity *in vivo* [38]. We hypothesized that in the Lipo-GA formulation, as the drug is loaded inside the liposomes with no burst release in the medium, the hemolytic toxicity would be reduced. In Fig. 3, complete hemolysis of human and sheep RBCs was observed 1 h post incubation with free GA (40 µg GA/mL + 44 µg arginine/mL), whereas Lipo-GA (40 or 200 µg GA/mL) only resulted in mild hemolysis (<7%), which was comparable with negative controls including the arginine solution (44 µg arginine/mL) and empty liposomes (1 mg total lipid/mL). The tested concentrations were based on the estimated C₀ after an i.v. dose of free GA at 4 mg/kg and Lipo-GA at 4 mg/kg or 20 mg/kg. The data suggest Lipo-GA displayed little acute hemolytic toxicity, while free GA could induce significant hematological toxicity, such as anemia.

3.4. PK study

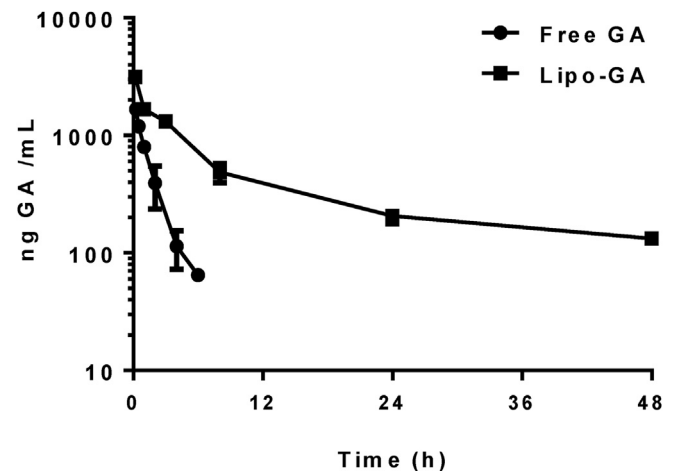
Since Lipo-GA exhibited no burst release when incubated with

Table 3
Characterization of Lipo-GA.

	Lipid composition	Drug/lipid (w/w)	Size (nm)	PDI	Loading efficiency (%)	DMSO (ppm)
Lipo-GA	DOPC/Chol/DSPE-mPEG2K (85/10/5, mol%)	1/5	74.81 ± 0.69	0.081 ± 0.04	99.21 ± 1.31	<0.55

**Fig. 2.** Cryo-TEM images of empty liposomes (DOPC/Chol/DSPE-PEG2K, 85/10/5 by mol%) (A) and Lipo-GA (B).**Fig. 3.** *In vitro* hemolysis test. Data = mean ± SD (n = 3).

serum, it was anticipated that Lipo-GA would displayed prolonged PK relative to free GA. Free GA and Lipo-GA were i.v. injected into BALB/c mice. Plasma was collected at selected time points and analyzed for GA using LC-MS/MS. The plasma profiles of free GA and Lipo-GA in mice were shown in Fig. 4. Free GA was rapidly eliminated from the plasma and the concentration was below the detection limit 6 h post injection (<60 ng/mL). Lipo-GA, on the other hand, displayed an increased plasma concentration at any given time compared to free GA with a reduced rate of elimination. The plasma concentration of Lipo-GA at 48 h post injection was still above 100 ng/mL. PK parameters were obtained by fitting the plasma profile with the non-compartmental model and are presented in Table 4. The half-life of Lipo-GA was significantly extended in comparison with free GA with an 18-fold increase (1.33 h vs 18.62 h). Lipo-GA also exhibited 20-fold higher mean residence time, 7.5-fold higher area under the curve ($AUC_{0-\infty}$), and 10-fold decreased clearance, confirming its prolonged circulation relative to free GA.

**Fig. 4.** PK profiles of free GA and Lipo-GA in BALB/c mice. Data = mean ± SD (n = 4).**Table 4**

Non-compartmental PK analysis of plasma profiles of free GA and Lipo-GA. C_{max} : maximum plasma concentration. $T_{1/2}$: half-life. $AUC_{0-\infty}$: area under the curve. Cl: clearance. Vd: volume of distribution. MRT: mean residence time.

	Free GA	Lipo-GA
C_{max} (µg/mL)	1.66 ± 0.02	3.14 ± 0.25
$AUC_{0-\infty}$ (µg/mL)	2.63 ± 0.24	19.6 ± 1.92
$T_{1/2}$ (h)	1.33 ± 0.28	18.62 ± 3.98
MRT (h)	1.59 ± 0.16	21.42 ± 1.32
Cl (mL/h/kg)	72.91 ± 7.05	8.72 ± 0.98
Vz (mL)	140.04 ± 26.06	231.19 ± 34.53

3.5. Antitumor efficacy in mice tumor models

The *in vitro* cytotoxicity of Lipo-GA was comparable to free GA in both EMT6 and B16F10 cells with an IC_{50} of 0.2–1.2 µM upon 3 days

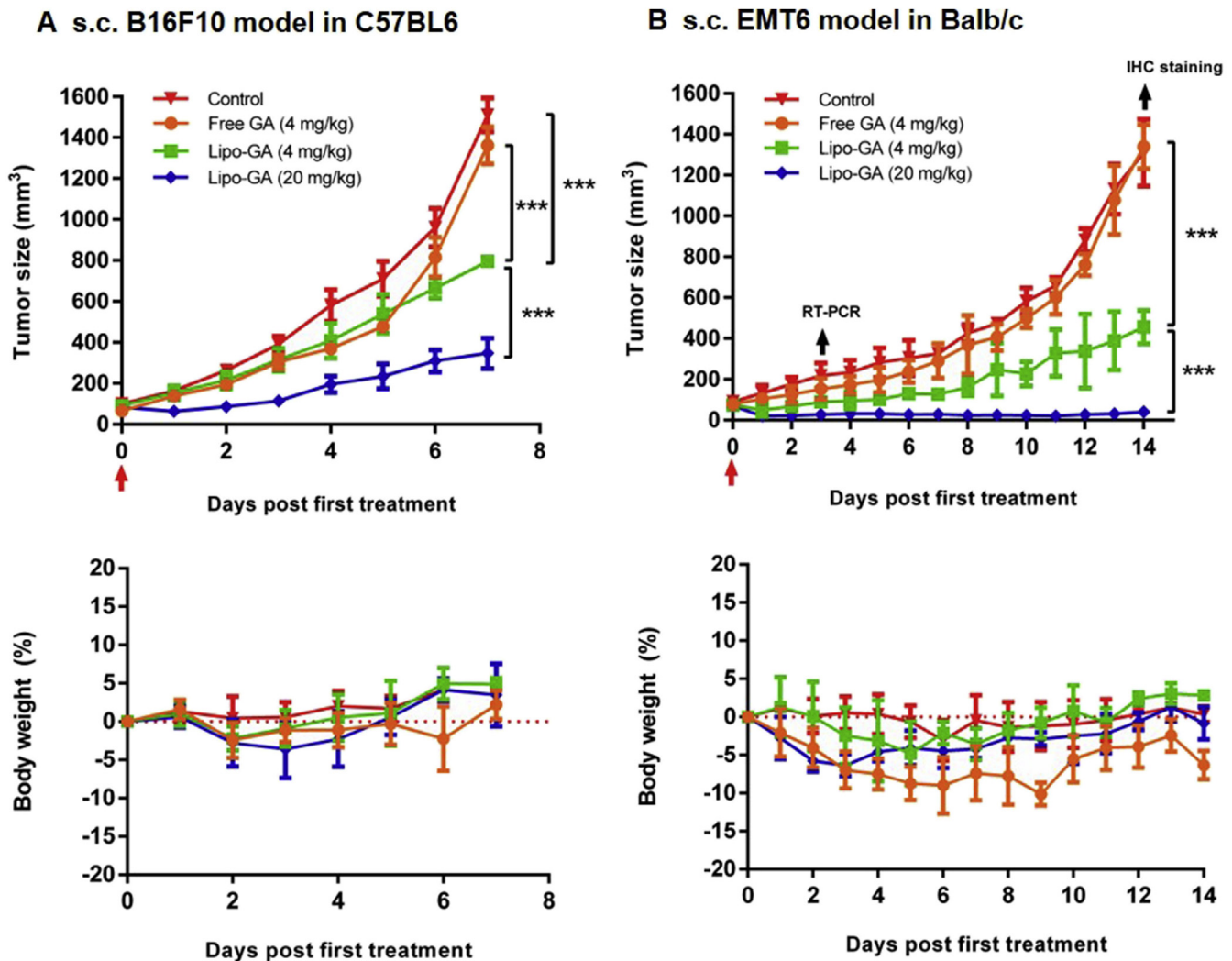


Fig. 5. Antitumor efficacy and safety of free GA and Lipo-GA in B16F10 (A) and EMT-6 (B) tumor models. Upper panel: tumor size; lower panel: body weight change during therapy. Data = mean \pm SD (n = 5–6).

of incubation (Supplementary Fig. 3). To evaluate the antitumor activity of Lipo-GA compared to free GA, mice with s.c. tumor ($\sim 100 \text{ mm}^3$) were randomly divided into 4 groups, and treated with control (empty liposome), free GA (4 mg GA/kg), or Lipo-GA (4 or 20 mg GA/kg) via tail vein injection (one dose). The dose was selected based on the previous report showing that 4 mg/kg of free GA was a non-toxic therapeutic dose that induced significant antitumor efficacy against a panel of human xenograft tumor models in mice [22,39,40].

In this study, we compared the one dose efficacy of free GA and Lipo-GA in murine syngeneic tumor models. In B16F10 melanoma model, free GA (4 mg GA/kg) did not show any significant antitumor effect relative to the negative control, whereas Lipo-GA at 4 mg GA/kg and 20 mg GA/kg significantly inhibited tumor growth by 47.5% ($p < 0.001$) and 77.1% ($p < 0.001$), respectively, on day 7 (Fig. 5A). The high-dose Lipo-GA (20 mg/kg) was significantly more efficacious than the low dose formulation (4 mg/kg). Similar results were obtained in the EMT6 breast tumor model, one dose treatment of Lipo-GA at 4 mg GA/kg and 20 mg GA/kg inhibited the tumor growth by 65.9% and 97%, respectively, while free GA at 4 mg/kg exhibited little efficacy (Fig. 5B). It is worth mentioning that the high dose Lipo-GA (20 mg/kg) induced significant tumor regression with only one dose and the tumor size stayed completely inhibited

for at least 12 days, followed by a slow rebound of the tumors. Preliminary safety of GA therapies was monitored by measuring the mice body weight. As shown in the lower panel of Fig. 5, no significant weight loss was observed in both tumor models after all treatments except for free GA and the high dose Lipo-GA in the BALB/c model. The body weight loss in the Lipo-GA group was mild ($< 5\%$) and was only significant on day 2 and 3, while free GA caused moderate weight loss (5–10%) during a period of time from day 2–10. The data in Fig. 5 indicate that Lipo-GA was a safer and more efficacious formulation compared to free GA.

In recent studies, GA has been shown *in vitro* as an effective inhibitor against STAT3 and NF- κ B, thereby downregulating the expression of a series of downstream genes related to angiogenesis, cell proliferation, and apoptosis, including Bcl-2, HIF-1 α , and VEGF-A [13,41]. In our study with the EMT6 tumor model, 3 days after the treatment, tumors were collected for analysis of these oncogenes by RT-PCR. As shown in Fig. 6, free GA (4 mg/kg) only mildly reduced the mRNA level of Bcl-2 and VEGF-A by 10% relative to the negative control. At the matched dose (4 mg GA/kg), Lipo-GA reduced the mRNA level of Bcl-2 by 40%, HIF-1 α by 36%, VEGF-A by 15%, and Stat3 by 38%. The effects were significantly stronger with Lipo-GA compared to free GA in all the analyzed genes except VEGF-A. Increasing the Lipo-GA dose to 20 mg/kg further increased

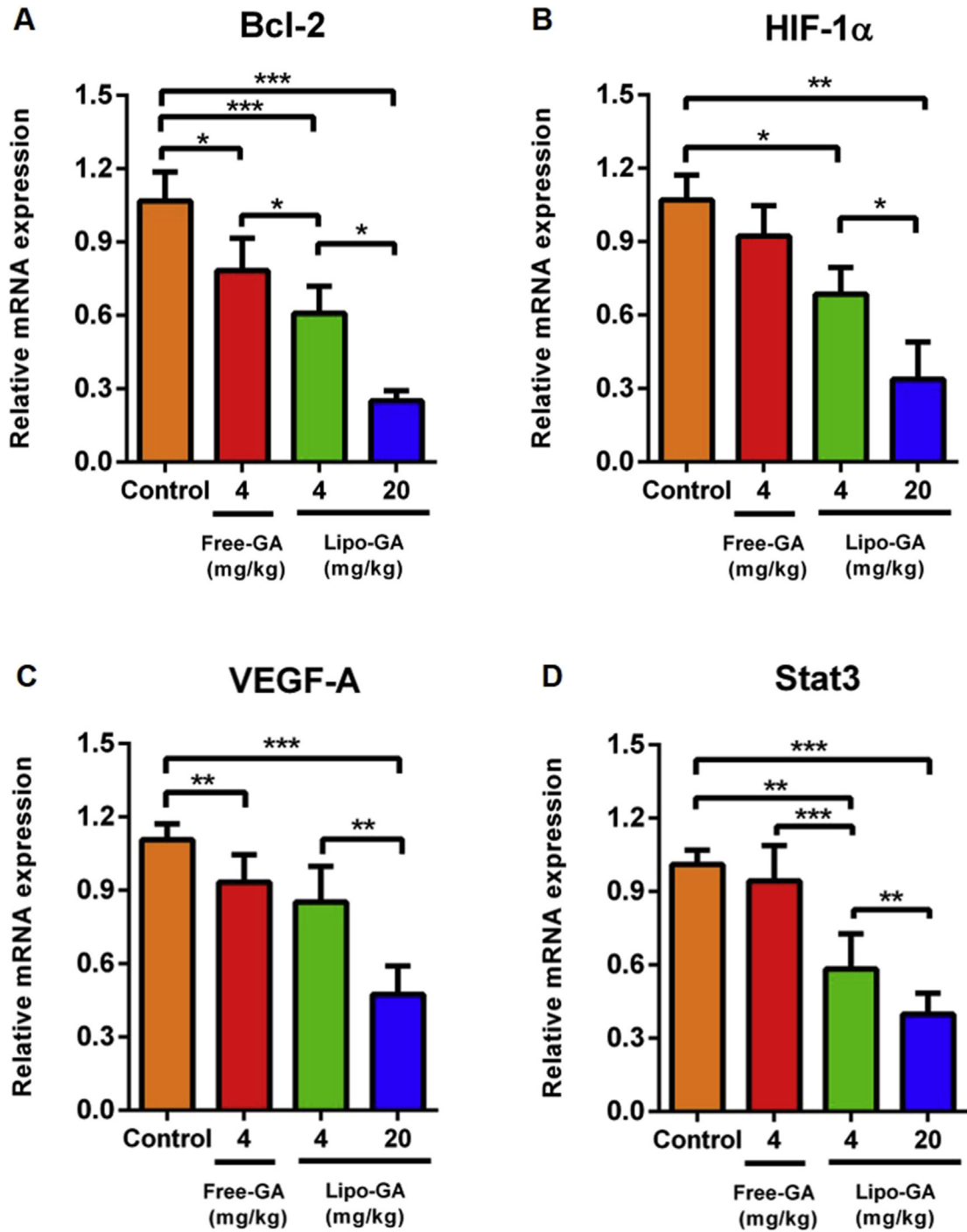


Fig. 6. Relative mRNA expression of genes 3 d post-treatment of various formulations in EMT6 tumor model. (A) Bcl-2, (B) HIF-1 α , (C) VEGF-A, and (D) Stat3. Data represent mean \pm SD (n = 3) (*P \leq 0.05, **p < 0.01, ***p < 0.001).

the activity in inhibiting these oncogenes by reducing the mRNA level of Bcl-2 by 75%, HIF-1 α by 70%, VEGF-A by 55%, and Stat3 by 60%. The data confirmed that Lipo-GA exhibited increased biological activity compared to free GA, and the effect was dose dependent.

Two weeks after various treatments, the EMT6 tumors were collected and analyzed for expression of Ki67, CD31, and NF- κ B p65. The H&E staining (Fig. 7A) clearly showed significant difference in morphology among the tumors after different therapies. The high-dose Lipo-GA group displayed the most significantly altered tumor

structure, indicating the highest antitumor efficacy. Ki67 is a proliferative marker and was highly expressed in the control tumor (65% positive, Fig. 7B). While free GA (4 mg/kg) showed no significant effect in reducing Ki67, Lipo-GA (4 mg/kg and 20 mg/kg) down-regulated Ki67 in the tumors to only 38% and 20%, respectively. Overexpression of CD31 is commonly seen in rapidly growing tumors with active angiogenesis [42]. As shown in Fig. 7A&C, free GA (4 mg/kg) did not exhibit significant anti-angiogenesis effect, whereas Lipo-GA at 4 mg/kg and 20 mg/kg reduced CD31 expression in the tumors by 50% and 75%,

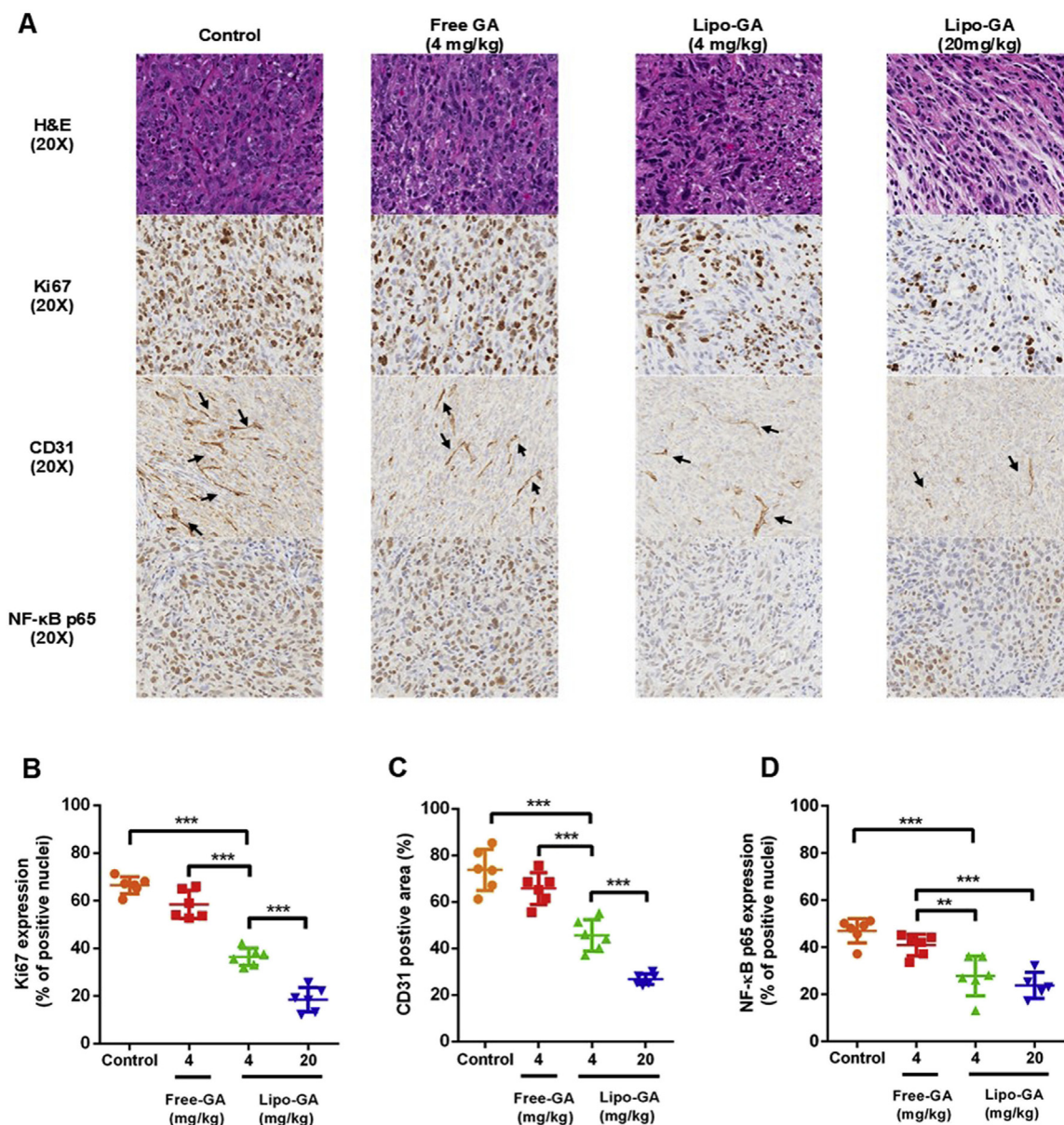


Fig. 7. Histological analysis of EMT6 tumor 14 days post-treatment with various GA formulations. Representative images of immunohistochemically stained tumor sections (A). Quantitative results of Ki67 (B), CD31 (C) and NF- κ B p65 (D) expression in the tumors. Data represent mean \pm SD (n = 6 images randomly selected from 5 tumors per group) (**p < 0.01, ***p < 0.001).

respectively, in comparison with the control. RelA, a subunit in the NF- κ B complexes, is exposed when the complexes are activated and translocated into the nucleus. RelA can be recognized by the NF- κ B p65 antibody to identify the active form of NF- κ B. As shown in Fig. 7A&D, free GA (4 mg/kg) displayed no activity in inhibiting NF- κ B in the tumor, while Lipo-GA (4 mg/kg and 20 mg/kg) reduced the active form of NF- κ B by 40–50% compared to the negative control. However, in this case, there was no dose effect of Lipo-GA in inhibiting NF- κ B. These IHC results were consistent with the tumor growth inhibition data. The increased antitumor activity of a single dose Lipo-GA relative to free GA could be mainly due to its increased half-life and systemic exposure (AUC), so that the effect of Lipo-GA could be enhanced and prolonged (up to 2 weeks in the EMT6 model). Additionally, since the hemolytic toxicity is reduced by the liposomal formulation, Lipo-GA could be safely given at a higher dose, leading to further enhanced antitumor efficacy.

Active loading of hydrophobic drugs into liposomes has been challenging [43–50]. Three such approaches have been developed recently [7,47,48,51]. The first strategy is prodrug-based approach [47]. Docetaxel was first chemically modified with an ionizable piperazine group via esterification, which increased the drug solubility at pH 5 and allowed the prodrug to permeate into the aqueous core, become ionized and form complexes with sulfate ions at a high drug-to-lipid ratio (0.4, w/w). However, this method required chemical modification of the drug. The second approach involved using a chemically modified cyclodextran with an ionizable alkyl amino group as a solubilizer and a membrane shuttle for an insoluble drug. The drug could be incorporated inside the modified cyclodextran, which could cross the lipid bilayer and become ionized and locked inside the low pH liposomal core [48]. The highest drug-to-lipid ratio achieved with this method was 0.1 (w/w). However, this method required a long process of

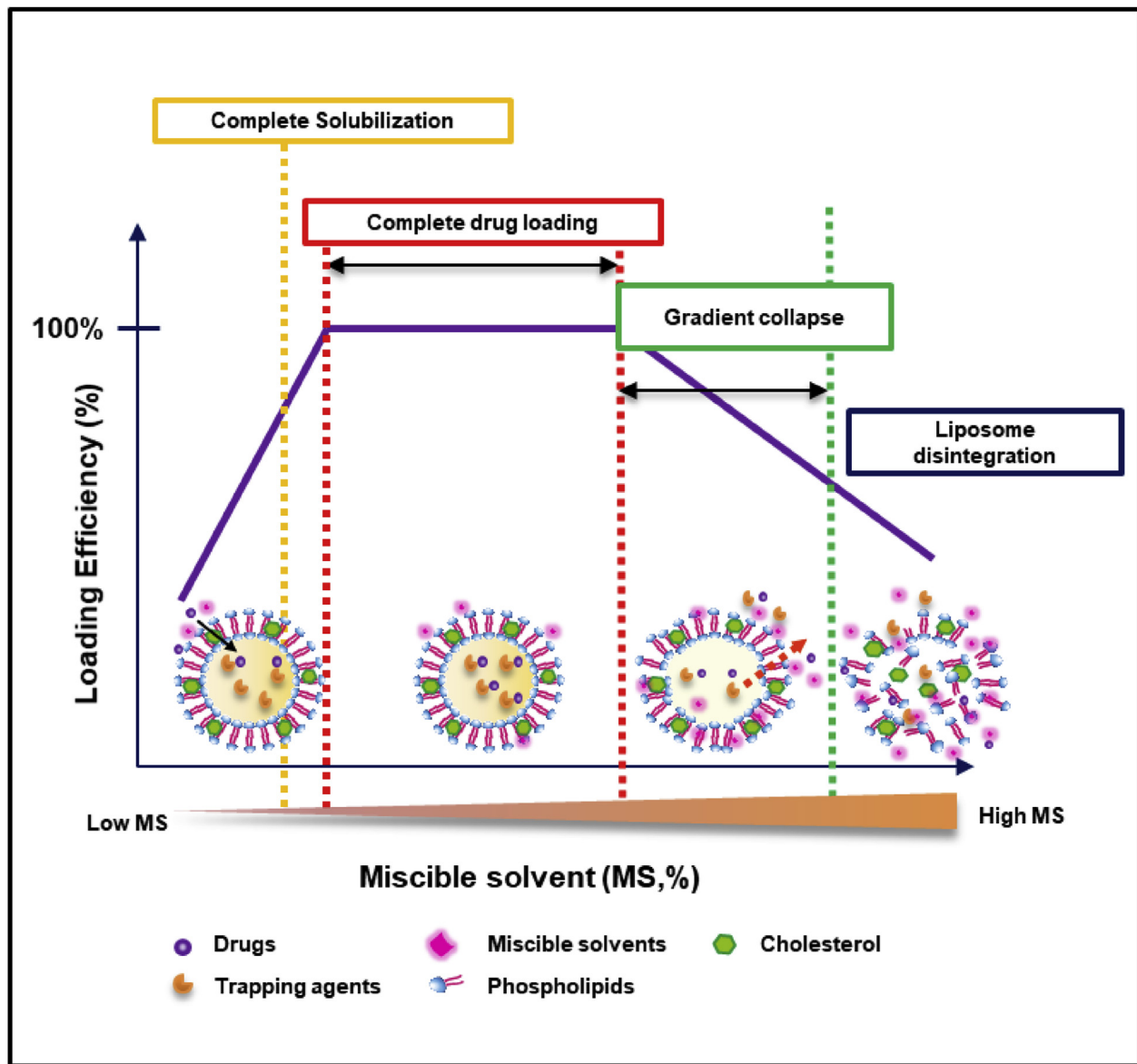


Fig. 8. The solvent effect on drug loading in the SALT system.

preparation (55 °C, 36–48 h). The final product would also contain the modified cyclodextran with an unknown safety profile. Very recently, including a solvent during the loading process has been shown to promote active loading of poorly water soluble drugs into liposomes [7,51,52]. Previous work from the Bally lab showed that 10–15% (v/v) ethanol could be used as a permeability enhancer to increase loading efficiency of anthracyclines (e.g. doxorubicin, idarubicin, and so on) in Chol-free liposomes (DSPC/DSPE-mPEG2K, 95/5, mol%) [52]. Complete drug loading could be achieved at a temperature (40 °C) lower than the phase transition temperature of the major lipid (DSPC, T_c: 55 °C). However, heating was still required with the Bally method. Additionally, it was not demonstrated whether this method could be applied for Chol-containing liposomes for active loading, and the optimal EtOH concentration was not identified. The Szoka group recently demonstrated that 2–10% (v/v) DMSO could facilitate high drug encapsulation (>90%) of a poorly water soluble drug (carfilzomib; logP 3.77) at a drug-to-lipid ratio of 0.12 (w/w). Under their specific conditions, carfilzomib was not completely soluble in the loading mixture [51]. With this

method, while high drug encapsulation could be achieved at room temperature for liposomes composed of a low transition temperature lipid (POPC, T_c: –2 °C), heating (65 °C) was required for those prepared with a high phase transition temperature lipid (DSPC, T_c: 55 °C). On the contrary, in the SALT system, a sufficient amount of solvent was included in the loading mixture to completely dissolve the drug and promote its loading into the liposomes composed of DSPC/Chol at room temperature at a drug-to-lipid ratio of >0.1 (w/w). The solvent could be efficiently removed from the final product by dialysis (<0.55 ppm upon 2 h dialysis) or tangential flow filtration [53]. The resulting liposomal drug exhibited superior stability and improved PK relative to the free drug. This platform is simple and highly flexible, working for a wide range of compounds and water miscible solvents. The loading can be completed in 30 min at room temperature, which is highly favorable for heat-sensitive drugs and large-scale manufacturing with no need of a delicate heating system to ensure homogenous heating. With this technology, the drug-to-lipid ratio that could be reached (0.1–0.2, w/w) was 50 times higher than that achieved by the passive loading

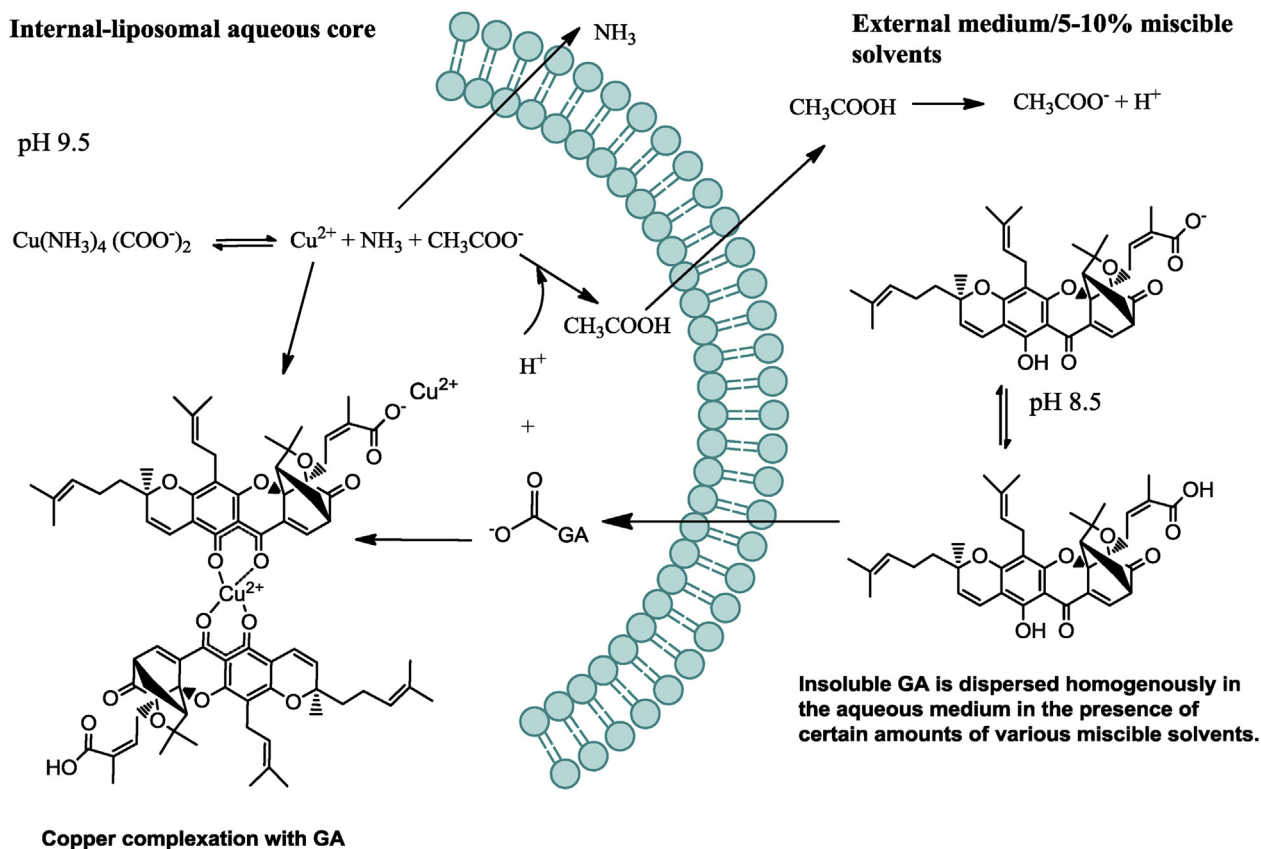


Fig. 9. Proposed mechanism of GA loading using basified copper acetate.

method [54,55]. In this study, we also examined the optimal range of solvents for compete drug loading at room temperature. The data showed that just complete solubilization of the compound was not enough, and a slightly extra amount of the solvent was needed, possibly to increase the membrane permeability to facilitate drug permeation through the lipid bilayer into the liposomal core at room temperature. The upper limit of the optimal amount of solvent must be below that for inducing bilayer instability, which resulted in the loss of the loading gradient. This working model is proposed and summarized in Fig. 8. The model suggests that the solvent used in the SALT is both a drug solubilizer and a membrane permeability enhancer. In the standard active loading method, heating is often used to increase the bilayer permeability. Indeed, when heating is applied in the SALT system, a less amount of solvent would be needed for complete loading, but in the meantime, the upper limit of the solvent was also decreased (data not shown). The data are consistent with the reports from the Bally lab and the Szoka team, supporting that the solvent used in SALT increased the bilayer permeability.

GA has shown significant antitumor efficacy in many studies [41,56–59]. However, its clinical application is limited due to its poor solubility (<5 µg/mL) and rapid drug clearance (half-life < 4 h in rat) [20,21]. Various nanoparticle delivery systems have been utilized to incorporate GA in the hydrophobic compartment to increase the solubility [22,25,26,60,61]. However, the stability of these GA-loaded nano-formulations was poor even in serum-free media (>40% release in 72 h). As the drug release was rapid, the circulation half-life was only marginally increased by <2-fold at best [25], and the improvement in efficacy for these delivery systems relative to free GA was only minimal.

To develop a stable liposomal formulation for GA, our strategy

was to employ the SALT to effectively encapsulate GA, and optimize the loading gradient and lipid composition to stably retain the drug. The optimal loading gradient and lipid composition were found to be basified copper acetate and DOPC/Chol/DSPE-mPEG2K (85/10/5, mol%), respectively. The proposed active loading mechanism for this formulation is depicted in Fig. 9. The miscible solvent dissolves GA into individual molecules and facilitates permeation of the uncharged form of GA into the liposomal core, where the basic pH (9.5) promotes de-protonation of GA to lock this ionized form inside the liposomes. Additionally, Cu^{2+} ions in the liposomal core form complexes with GA molecules, preventing it from leaking out. This formulation retained almost 100% of GA when incubated with 50% serum at 37 °C for 24 h, a prerequisite for prolonged PK. The ammonia (permeability coefficient $P = 6.6 \cdot 10^{-4}$ cm/s) and acetic acid ($P = 0.13$ cm/s) dissociated from basified copper acetate then diffuse out of the liposomes [62,63]. This equilibrated mechanism is anticipated to drive active and efficient loading of GA and maintain the stability. Indeed, in our attempts of using other salts of copper as the loading gradient, the liposomal drug retention was inferior to the basified copper acetate, including 100 mM copper gluconate/220 mM triethanolamine (TEA, pH 7.4), 250 mM basified copper sulfate (pH 9.5), and 250 mM copper sulfate (pH 4.0), shown in Supplementary Fig. 4A and B, suggesting the stability of liposomal GA may be primarily attributed to both the counterions and the inside pH [64]. To the best of our knowledge, this metal ion gradient has never been used before for loading drugs, and the combination of the basified copper loading and DOPC formulation yielded a stable liposomal formulation for GA, which displayed prolonged PK relative to free GA. In fact, this was also the first reported liposomal formulation for GA prepared by active loading that displayed extended blood circulation, to the best of our knowledge.

As a result, this Lipo-GA formulation displayed increased anti-tumor activity after only one single i.v. dose in two aggressive syngeneic tumor models in mice. This formulation also demonstrated unique antitumor mechanism by simultaneously inhibiting multiple oncogenes, including NF- κ B, Bcl-2, Stat3, HIF-1 α , and VEGF-A, leading to significant anti-proliferation and anti-angiogenesis in the treated tumor with significant tumor regression. It is worth mentioning that there are still no effective and safe drugs approved for deactivating many of those targets that Lipo-GA effectively inhibited, including NF- κ B, Bcl-2, Stat3, and HIF-1 α . Therefore, the potential of Lipo-GA in augmenting the current cancer therapy is very significant.

4. Conclusion

Through a comprehensive study, our data support that the SALT is a flexible platform for developing effective and stable liposomal formulations for a wide range of poorly water soluble drugs. Our study also delineated the roles of the solvents used in the SALT system, including dissolving the compound and increasing the membrane permeation at room temperature. We then further utilized the SALT, and optimized the loading gradient as well as liposomal composition, to develop a stable liposomal formulation for GA. Compared to free GA, Lipo-GA displayed reduced hemolytic toxicity, prolonged PK, and enhanced efficacy against multiple tumor models by simultaneously inhibiting multiple oncogenes.

Acknowledgements

The research was supported by grants from the Canadian Institutes of Health Research, the Natural Science and Engineering Research Council in Canada (NSERC), and the Faculty of Pharmaceutical Sciences at University of British Columbia (UBC). W.L.T. is supported by Frederick Banting and Charles Best Canada Graduate Scholarship from CIHR as well as Four Year Fellowship (4YF) Tuition Award from the UBC. S.D.L. received the CIHR New Investigator Salary Award and the Angiotech Professorship in Drug Delivery. The authors acknowledge the Wax-it Histology Services Inc for tissue staining, and image acquisition, and analysis. The authors acknowledge Mr. Fulong Wong and Dr. Nobuhito Hamano for technical supports for RT-PCR and i.v. injections.

Appendix A. Supplementary data

Supplementary data related to this article can be found at <https://doi.org/10.1016/j.biomaterials.2018.03.004>.

References

- [1] J.E. Lancet, J.E. Cortes, D.E. Hogge, M.S. Tallman, T.J. Kovacs, L.E. Damon, R. Komrokji, S.R. Solomon, J.E. Kolitz, M. Cooper, A.M. Yeager, A.C. Louie, E.J. Feldman, Phase 2 trial of CPX-351, a fixed 5:1 molar ratio of cytarabine/daunorubicin, vs cytarabine/daunorubicin in older adults with untreated AML, *Blood* 123 (21) (2014) 3239–3246.
- [2] E. Alphandéry, P. Grand-Dewyse, R. Lefèvre, C. Mandawala, M. Durand-Dubief, Cancer therapy using nanoformulated substances: scientific, regulatory and financial aspects, *Expert Rev. Anticancer Ther.* 15 (10) (2015) 1233–1255.
- [3] C.M. Dawidczyk, C. Kim, J.H. Park, L.M. Russell, K.H. Lee, M.G. Pomper, P.C. Searson, State-of-the-art in design rules for drug delivery platforms: lessons from FDA-approved nanomedicines, *J. Contr. Release* 187 (2014) 133–144.
- [4] F.N.U.A.u. Rahman, S. Ali, M.W. Saif, Update on the role of nanoliposomal irinotecan in the treatment of metastatic pancreatic cancer, *Therap. Adv. Gastroenterol.* 10 (7) (2017) 563–572.
- [5] Q. Xu, Y. Tanaka, J.T. Czernuszka, Encapsulation and release of a hydrophobic drug from hydroxyapatite coated liposomes, *Biomaterials* 28 (16) (2007) 2687–2694.
- [6] P. Kan, C.-W. Tsao, A.-J. Wang, W.-C. Su, H.-F. Liang, A liposomal formulation able to incorporate a high content of paclitaxel and exert promising anticancer effect, *J. Drug Deliv.* 2011 (2011).
- [7] W.-L. Tang, W.C. Chen, A. Roy, E. Undzys, S.-D. Li, A simple and improved active loading method to efficiently encapsulate staurosporine into lipid-based nanoparticles for enhanced therapy of multidrug resistant cancer, *Pharmaceut. Res.* 33 (5) (2016) 1104–1114.
- [8] Z.-Q. Wu, Q.-L. Guo, Q.-D. You, L. Zhao, H.-Y. Gu, Gambogic acid inhibits proliferation of human lung carcinoma SPC-A1 cells in vivo and in vitro and represses telomerase activity and telomerase reverse transcriptase mRNA expression in the cells, *Biol. Pharm. Bull.* 27 (11) (2004) 1769–1774.
- [9] X. Li, S. Liu, H. Huang, N. Liu, C. Zhao, S. Liao, C. Yang, Y. Liu, C. Zhao, S. Li, X. Lu, C. Liu, L. Guan, K. Zhao, X. Shi, W. Song, P. Zhou, X. Dong, H. Guo, G. Wen, C. Zhang, L. Jiang, N. Ma, B. Li, S. Wang, H. Tan, X. Wang, Q.P. Dou, J. Liu, Gambogic acid is a tissue-specific proteasome inhibitor in vitro and in vivo, *Cell Rep.* 3 (1) (2013) 211–222.
- [10] M. Ishaq, M.A. Khan, K. Sharma, G. Sharma, R.K. Dutta, S. Majumdar, Gambogic acid induced oxidative stress dependent caspase activation regulates both apoptosis and autophagy by targeting various key molecules (NF- κ B, Beclin-1, p62 and NBR1) in human bladder cancer cells, *Biochim. Biophys. Acta* 1840 (12) (2014) 3374–3384.
- [11] J. Yu, Q.-L. Guo, Q.-D. You, L. Zhao, H.-Y. Gu, Y. Yang, H.-w. Zhang, Z. Tan, X. Wang, Gambogic acid-induced G2/M phase cell-cycle arrest via disturbing CDK7-mediated phosphorylation of CDC2/p34 in human gastric carcinoma BGC-823 cells, *Carcinogenesis* 28 (3) (2007) 632–638.
- [12] T. Yi, Z. Yi, S.-G. Cho, J. Luo, M.K. Pandey, B.B. Aggarwal, M. Liu, Gambogic acid inhibits angiogenesis and prostate tumor growth by suppressing vascular endothelial growth factor receptor 2 signaling, *Canc. Res.* 68 (6) (2008) 1843–1850.
- [13] S. Prasad, M.K. Pandey, V.R. Yadav, B.B. Aggarwal, Gambogic acid inhibits STAT3 phosphorylation through activation of protein tyrosine phosphatase SHP-1: potential role in proliferation and apoptosis, *Canc. Prev. Res.* 4 (7) (2011) 1084–1094.
- [14] T. Yi, Z. Yi, S.-G. Cho, J. Luo, M.K. Pandey, B.B. Aggarwal, M. Liu, Gambogic acid inhibits angiogenesis and prostate tumor growth by suppressing VEGFR2 signaling, *Cancer Research* 68 (6) (2008) 1843–1850.
- [15] B.V.R. Cascao, H. Raquel, A. Neves-Costa, N. Figueiredo, V. Gupta, J. Fonseca, O. Eurico, L. Ferreira Moita, Potent anti-inflammatory and antiproliferative effects of gambogic acid in a rat model of antigen-induced arthritis, *Mediat. Inflamm.* 2014 (2014) 7.
- [16] M.-S. Park, N.-H. Kim, C.-W. Kang, C.-W. Oh, G.-D. Kim, Antimetastatic effects of gambogic acid are mediated via the actin cytoskeleton and NF- κ B pathways in SK-HEP1 cells, *Drug Dev. Res.* 76 (3) (2015) 132–142.
- [17] S. Wang, L. Wang, M. Chen, Y. Wang, Gambogic acid sensitizes resistant breast cancer cells to doxorubicin through inhibiting P-glycoprotein and suppressing survivin expression, *Chem. Biol. Interact.* 235 (Supplement C) (2015) 76–84.
- [18] C. Wang, W. Wang, C. Wang, Y. Tang, H. Tian, Combined therapy with EGFR TKI and gambogic acid for overcoming resistance in EGFR-T790M mutant lung cancer, *Oncol. Lett.* 10 (4) (2015) 2063–2066.
- [19] G. Xia, H. Wang, Z. Song, Q. Meng, X. Huang, X. Huang, Gambogic acid sensitizes gemcitabine efficacy in pancreatic cancer by reducing the expression of ribonucleotide reductase subunit-M2 (RRM2), *J. Exp. Clin. Oncol.* 36 (2017) 107.
- [20] K. Hao, X.-Q. Liu, G.-J. Wang, X.-P. Zhao, Pharmacokinetics, tissue distribution and excretion of gambogic acid in rats, *Eur. J. Drug Metab. Pharmacokinet.* 32 (2) (2007) 63–68.
- [21] Z. Zheng, W. Ou, X. Zhang, Y. Li, Y. Li, UHPLC-MS method for determination of gambogic acid and application to bioavailability, pharmacokinetics, excretion and tissue distribution in rats, *Biomed. Chromatogr.* 29 (10) (2015) 1581–1588.
- [22] L. Cai, N. Qiu, M. Xiang, R. Tong, J. Yan, L. He, J. Shi, T. Chen, J. Wen, W. Wang, L. Chen, Improving aqueous solubility and antitumor effects by nanosized gambogic acid-mPEG(2000) micelles, *Int. J. Nanomed.* 9 (2014) 243–255.
- [23] R. Doddapaneni, K. Patel, I.H. Owaid, M. Singh, Tumor neo-vasculature targeted cationic PEGylated liposomes of gambogic acid for the treatment of triple negative breast cancer, *Drug Deliv.* 23 (4) (2016) 1232–1241.
- [24] Z. Zhang, H. Qian, M. Yang, R. Li, J. Hu, L. Li, L. Yu, B. Liu, X. Qian, Gambogic acid-loaded biomimetic nanoparticles in colorectal cancer treatment, *Int. J. Nanomed.* 12 (2017) 1593–1605.
- [25] D. Yin, Y. Yang, H. Cai, F. Wang, D. Peng, L. He, Gambogic acid-loaded electrosprayed particles for site-specific treatment of hepatocellular carcinoma, *Mol. Pharm.* 11 (11) (2014) 4107–4117.
- [26] D. Zhang, Z. Zou, W. Ren, H. Qian, Q. Cheng, L. Ji, B. Liu, Q. Liu, Gambogic acid-loaded PEG-PCL nanoparticles act as an effective antitumor agent against gastric cancer, *Pharmaceut. Dev. Technol.* (2017) 1–8.
- [27] J.C.M. Stewart, Colorimetric determination of phospholipids with ammonium ferrioxalate, *Anal. Biochem.* 104 (1) (1980) 10–14.
- [28] A.K.K. Leung, Y.Y.C. Tam, S. Chen, I.M. Hafez, P.R. Cullis, Microfluidic mixing: a general method for encapsulating macromolecules in lipid nanoparticle systems, *J. Phys. Chem. B* 119 (28) (2015) 8698–8706.
- [29] J.A. Kulkarni, Y.Y.C. Tam, S. Chen, Y.K. Tam, J. Zaifman, P.R. Cullis, S. Biswas, Rapid synthesis of lipid nanoparticles containing hydrophobic inorganic nanoparticles, *Nanoscale* 9 (36) (2017) 13600–13609.
- [30] T. Li, L. Zhang, L. Tong, Q. Liao, High-throughput salting-out-assisted homogeneous liquid–liquid extraction with acetonitrile for determination of baicalin in rat plasma with high-performance liquid chromatography, *Biomed. Chromatogr.* 28 (5) (2014) 648–653.
- [31] L. Clary, G. Verderone, C. Santaella, P. Vierling, Membrane permeability and

- stability of liposomes made from highly fluorinated double-chain phosphocholines derived from diaminoopropanol, serine or ethanolamine, *Biochim. Biophys. Acta Biomembr.* 1328 (1) (1997) 55–64.
- [32] A.M. Firsov, E.A. Kotova, E.A. Korepanova, A.N. Osipov, Y.N. Antonenko, Peroxidative permeabilization of liposomes induced by cytochrome c/cardiolipin complex, *Biochim. Biophys. Acta Biomembr.* 1848 (3) (2015) 767–774.
- [33] N. Dos Santos, L.D. Mayer, S.A. Abraham, R.C. Gallagher, K.A.K. Cox, P.G. Tardi, M.B. Bally, Improved retention of idarubicin after intravenous injection obtained for cholesterol-free liposomes, *Biochim. Biophys. Acta Biomembr.* 1561 (2) (2002) 188–201.
- [34] G.J.R. Charrois, T.M. Allen, Drug release rate influences the pharmacokinetics, biodistribution, therapeutic activity, and toxicity of pegylated liposomal doxorubicin formulations in murine breast cancer, *Biochim. Biophys. Acta Biomembr.* 1663 (1–2) (2004) 167–177.
- [35] H.-I. Chang, M.-K. Yeh, Clinical development of liposome-based drugs: formulation, characterization, and therapeutic efficacy, *Int. J. Nanomed.* 7 (2012) 49–60.
- [36] A. Kheirloomoom, L.M. Mahakian, C.-Y. Lai, H.A. Lindfors, J.W. Seo, E.E. Paoli, K.D. Watson, E.M. Haynam, E.S. Ingham, L. Xing, R.H. Cheng, A.D. Borowsky, R.D. Cardiff, K.W. Ferrara, Copper-doxorubicin as a nanoparticle cargo retains efficacy with minimal toxicity, *Mol. Pharm.* 7 (6) (2010) 1948–1958.
- [37] A. Dicko, S. Kwak, A.A. Frazier, L.D. Mayer, B.D. Liboiron, Biophysical characterization of a liposomal formulation of cytarabine and daunorubicin, *Int. J. Pharm.* 391 (1) (2010) 248–259.
- [38] A. Lupescu, K. Jilani, C. Zelenak, M. Zbidah, N. Shaik, F. Lang, Induction of programmed erythrocyte death by gambogic acid, *Cell. Physiol. Biochem.* 30 (2) (2012) 428–438.
- [39] Q. Guo, Q. Qi, Q. You, H. Gu, L. Zhao, Z. Wu, Toxicological studies of gambogic acid and its potential targets in experimental animals, *Basic Clin. Pharmacol. Toxicol.* 99 (2) (2006) 178–184.
- [40] X. Li, S. Liu, H. Huang, N. Liu, C. Zhao, S. Liao, C. Yang, Y. Liu, C. Zhao, S. Li, X. Lu, C. Liu, L. Guan, K. Zhao, X. Shi, W. Song, P. Zhou, X. Dong, H. Guo, G. Wen, C. Zhang, L. Jiang, N. Ma, B. Li, S. Wang, H. Tan, X. Wang, Q.P. Dou, J. Liu, Gambogic acid is a tissue-specific proteasome inhibitor in vitro and in vivo, *Cell Rep.* 3 (1) (2013) 211–222.
- [41] K. Zhao, S. Zhang, X. Song, Y. Yao, Y. Zhou, Q. You, Q. Guo, N. Lu, Gambogic acid suppresses cancer invasion and migration by inhibiting TGFbeta1-induced epithelial-to-mesenchymal transition, *Oncotarget* 8 (16) (2017) 27120–27136.
- [42] D. Wang, C.R. Stockard, L. Harkins, P. Lott, C. Salih, K. Yuan, D. Buchsbaum, A. Hashim, M. Zayzafoon, R. Hardy, O. Hameed, W. Grizzle, G.P. Siegal, Immunohistochemistry in the evaluation of neovascularization in tumor xenografts, *Biotech. Histochem. Off. Pub. Biol. Stain Comm.* 83 (0) (2008) 179–189.
- [43] T. Shigehiro, T. Kasai, M. Murakami, S.C. Sekhar, Y. Tominaga, M. Okada, T. Kudoh, A. Mizutani, H. Murakami, D.S. Salomon, K. Mikuni, T. Mandai, H. Hamada, M. Seno, Efficient drug delivery of paclitaxel glycoside: a novel solubility gradient encapsulation into liposomes coupled with immunoliposomes preparation, *PLoS One* 9 (9) (2014) e107976.
- [44] R. Mukthavaram, P. Jiang, R. Saklecha, D. Simberg, I.S. Bharati, N. Nomura, Y. Chao, S. Pastorino, S.C. Pingle, V. Fogal, W. Wrasidlo, M. Makale, S. Kesari, High-efficiency liposomal encapsulation of a tyrosine kinase inhibitor leads to improved in vivo toxicity and tumor response profile, *Int. J. Nanomed.* 8 (2013) 3991–4006.
- [45] M. Yamauchi, H. Kusano, M. Nakakura, Y. Kato, Reducing the impact of binding of UCN-01 to human alpha1-acid glycoprotein by encapsulation in liposomes, *Biol. Pharm. Bull.* 28 (5) (2005) 1259–1264.
- [46] K. Park, Active liposomal loading of a poorly soluble ionizable drug, *J. Contr. Release* 162 (2) (2012) 475.
- [47] I.V. Zhigaltsev, G. Winters, M. Srinivasulu, J. Crawford, M. Wong, L. Amankwa, D. Waterhouse, D. Masin, M. Webb, N. Harasym, L. Heller, M.B. Bally, M.A. Ciufolini, P.R. Cullis, N. Maurer, Development of a weak-base docetaxel derivative that can be loaded into lipid nanoparticles, *J. Contr. Release* 144 (3) (2010) 332–340.
- [48] S. Sur, A.C. Fries, K.W. Kinzler, S. Zhou, B. Vogelstein, Remote loading of preencapsulated drugs into stealth liposomes, *Proc. Natl. Acad. Sci. U. S. A.* 111 (6) (2014) 2283–2288.
- [49] S. Modi, T.X. Xiang, B.D. Anderson, Enhanced active liposomal loading of a poorly soluble ionizable drug using supersaturated drug solutions, *J. Contr. Release* 162 (5) (2012) 330–339.
- [50] V. Joguparthi, T.X. Xiang, B.D. Anderson, Liposome transport of hydrophobic drugs: gel phase lipid bilayer permeability and partitioning of the lactone form of a hydrophobic camptothecin, DB-67, *J. Pharmaceut. Sci.* 97 (1) (2008) 400–420.
- [51] M.E. Hayes, C.O. Noble, F.C. Szoka, Remote loading of sparingly water-soluble drugs into liposomes, US Patent No, 2014/0220110 A1, 2014.
- [52] N. Dos Santos, K.A. Cox, C.A. McKenzie, F. van Baarda, R.C. Gallagher, G. Karlsson, K. Edwards, L.D. Mayer, C. Allen, M.B. Bally, pH gradient loading of anthracyclines into cholesterol-free liposomes: enhancing drug loading rates through use of ethanol, *Biochim. Biophys. Acta Biomembr.* 1661 (1) (2004) 47–60.
- [53] W.-L. Tang, W.-H. Tang, W.C. Chen, C. Diako, C.F. Ross, S.-D. Li, Development of a rapidly dissolvable oral pediatric formulation for mefloquine using liposomes, *Mol. Pharm.* 14 (6) (2017) 1969–1979.
- [54] M. Mahmud, A. Piwoni, N. Filiczak, M. Janicka, J. Gubernator, Long-circulating curcumin-loaded liposome formulations with high incorporation efficiency, stability and anticancer activity towards pancreatic adenocarcinoma cell lines in vitro, *PLoS One* 11 (12) (2016) e0167787.
- [55] K. Tschaikowsky, J.D. Brain, Staurosporine encapsulated into pH-sensitive liposomes reduces tnfr production and increases survival in rat endotoxin shock, *Shock* 1 (6) (1994) 401–407.
- [56] X. Shi, X. Lan, X. Chen, C. Zhao, X. Li, S. Liu, H. Huang, N. Liu, D. Zang, Y. Liao, P. Zhang, X. Wang, J. Liu, Gambogic acid induces apoptosis in diffuse large B-cell lymphoma cells via inducing proteasome inhibition, *Sci. Rep.* 5 (2015) 9694.
- [57] Q. Qi, N. Lu, C. Li, J. Zhao, W. Liu, Q. You, Q. Guo, Involvement of RECK in gambogic acid induced anti-invasive effect in A549 human lung carcinoma cells, *Mol. Carcinog.* 54 (Suppl 1) (2015) E13–E25.
- [58] L.H. Wang, J.Y. Yang, S.N. Yang, Y. Li, G.F. Ping, Y. Hou, W. Cui, Z.Z. Wang, W. Xiao, C.F. Wu, Suppression of NF-kappaB signaling and P-glycoprotein function by gambogic acid synergistically potentiates adriamycin -induced apoptosis in lung cancer, *Curr. Cancer Drug Targets* 14 (1) (2014) 91–103.
- [59] Y. Yang, X. Sun, Y. Yang, X. Yang, H. Zhu, S. Dai, X. Chen, H. Zhang, Q. Guo, Y. Song, F. Wang, H. Cheng, X. Sun, Gambogic acid enhances the radiosensitivity of human esophageal cancer cells by inducing reactive oxygen species via targeting Akt/mTOR pathway, *Tumour Biol* 37 (2) (2016) 1853–1862.
- [60] M. He, L. Ro, J. Liu, C.-C. Chu, Folate-decorated arginine-based poly(ester urea urethane) nanoparticles as carriers for gambogic acid and effect on cancer cells, *J. Biomed. Mater. Res.* 105 (2) (2017) 475–490.
- [61] R. Doddapaneni, K. Patel, I.H. Owaid, M. Singh, Tumor neovascularization-targeted cationic PEGylated liposomes of gambogic acid for the treatment of triple-negative breast cancer, *Drug Deliv.* 23 (4) (2016) 1232–1241.
- [62] S. Clerc, Y. Barenholz, Loading of amphipathic weak acids into liposomes in response to transmembrane calcium acetate gradients, *Biochim. Biophys. Acta Biomembr.* 1240 (2) (1995) 257–265.
- [63] G. Haran, R. Cohen, L.K. Bar, Y. Barenholz, Transmembrane ammonium sulfate gradients in liposomes produce efficient and stable entrapment of amphipathic weak bases, *Biochim. Biophys. Acta Biomembr.* 1151 (2) (1993) 201–215.
- [64] V. Joguparthi, B.D. Anderson, Liposomal delivery of hydrophobic weak acids: enhancement of drug retention using a high intraliposomal pH, *J. Pharmacol. Sci.* 97 (1) (2008) 433–454.